Available online at www.sciencedirect.com
SCIENCE DIRECT®
Pergamon
Cement and Concrete Research 34 (2004) 1725–1732
CEMENT AND CONCRETE RESEARCH

Phase studies of pozzolanic stabilized calcium silicate hydrates at 180 °C

K. Luke*

Halliburton Energy Services, 2600 South 2nd Street, Duncan, OK 73536, USA

Received 16 March 2004; accepted 6 May 2004

Abstract

Phase studies of calcium silicate hydrates formed at elevated temperature and pressure have been well documented. At 180 °C, the initially formed amorphous calcium silicate gel [C-S-H] transforms into well-defined crystalline phases, the stability of which is primarily dependent on the C/S ratio in the CaO-SiO_2-H_2O system and the hydrothermal conditions. Hillebrandite [C_2SH], α-dicalcium silicate hydrate [α-C_2SH] and β-tricalcium silicate [β-$C_6S_2H_3$] are predominantly the stable phases in the lime-rich part of the CaO-SiO_2-H_2O system and are typically associated with high permeability and compressive strength retrogression. Gyrolite [$C_2S_3H_{\sim 2}$], tobermorite [$C_5S_6H_5$], truscottite [$C_7S_{12}H_{\sim 3}$] and xonotlite [C_6S_6H] have all been reported to coexist stably in aqueous solution with silica in the silica-rich part of the CaO-SiO_2-H_2O system.

The addition of excess silica to the CaO-SiO_2-H_2O system is usually in the form of silicon dioxide [SiO_2], either as microsilica or quartz flour, which, in theory, should not affect the equilibrium chemistry. This has not been found to be the case, and metastable phases formed in the early stages of reaction modify the long-term stability and phase equilibrium. Pozzolanic materials that are predominantly alumino-silicates have also been investigated as a source of excess silica. Partial replacement of aluminum for silicon occurred, but had no apparent influence on the stability of the calcium silicate hydrates formed.

Keywords: Oil well cement; Hydration products; X-ray diffraction; Characterization; Hydrothermal

1. Introduction

The contributions of H.F.W. (Hal) Taylor to our understanding of the hydrothermal chemistry of calcium silicate hydrates are well known. In this paper, we present results on the effect of silica source on phase stability in the CaO-SiO_2-H_2O system at 180 °C, which fits well into the framework he so ably laid down.

The conditions of formation and stability of various calcium silicate hydrates at elevated temperatures and pressures are relevant to the hardening and durability in oil-well cementing. Phase equilibria in the CaO-SiO_2-H_2O system over a wide range of temperature, pressure and composition have been investigated [1–4]. At temperatures above approximately 120 °C, hydration products tend to crystallize. In the absence of reactive silica, C-S-H tends to be replaced by the crystalline phases in the lime-rich part of the CaO-SiO_2-H_2O system, namely, α-C_2SH [$Ca_2(HSiO_4)OH$], hillebrandite [$Ca_2SiO_3(OH)_2$] or, sometimes, at temperatures above 200 °C, C_3SH [$Ca_6Si_2O_7(OH)_6$]. These lime-rich phases are considered to be deleterious because they result in high permeability and low compressive strength. The incorporation of siliceous material to the cement produces numerous silica-rich crystalline phases, the stability of which is dependant on the initial C/S ratio, temperature and, to a lesser extent, pressure. Phases typically found are gyrolite [$Ca_4(Si_6O_{15})(OH)_2.3H_2O$] below about 330 °C, truscottite [$Ca_{14}Si_{24}O_{58}(OH)_8.2H_2O$] from about 180 °C to about 350 °C, 1.1 nm tobermorite [$Ca_5(OH)_2Si_6O_{16}.4H_2O$] from 120 °C to about 275 °C and xonotlite [$Ca_6(Si_6O_{17})(OH)_2$] from 165 °C to above about 385 °C. At temperatures below 180 °C, 1.1 nm tobermorite appears to be the more readily formed phase, and xonotlite is favored at temperatures of 180 °C and above. Gyrolite and truscottite are reported to form readily only if the siliceous material is in a reactive form [5–7]. These silica-rich phases in the CaO-SiO_2-H_2O system are generally associated with high compressive strengths [8,9]. Xonotlite generally gives about 20% to 25% lower strengths than tobermorite does Truscottite gives even lower strength but is less permeable than xonotlite [4].

In theory, the use of any pozzolanic material that reduces the C/S ratio to about 1.5 or less should prevent

* Tel.: +1-580-251-3353; fax: +1-450-251-4745.
E-mail address: karen.luke@halliburton.com (K. Luke).

0008-8846/$ – see front matter © 2004 Elsevier Ltd. All rights reserved.
doi:10.1016/j.cemconres.2004.05.021

the formation of the lime-rich phases in the $CaO-SiO_2-H_2O$ and prevent strength retrogression. It has been found, however, that this is typically not the case and that good strengths can only be obtained using quartz flour at approximately 35% to 40% by weight of cement, which gives a C/S ratio of 1.0–1.2. The use of course silica sand, condensed silica fume or other pozzolanic materials, such as fly ash, are reported to give poor strength development. The reasons for poor strength development in terms of equilibrium or nonequilibrium phase stabilities have been little investigated, but this present work attempts to explain these reasons.

2. Experimental

2.1. Starting materials

The ordinary Portland cement used in this study conforms to API Class H standard and is comparable with a coarsely ground ASTM Type V. The two fly ashes came from different base load power stations and, based on the sum of the $SiO_2 + Al_2O_3 + Fe_2O_3$, are classified as a Class F and Class C fly ash according to ASTM C618. Chemical analyses are provided in Table 1. CaO contents were determined as 7.14% and 25.61% by weight for the Class F and Class C fly ash, respectively. X-ray powder diffraction revealed that the crystalline, nonglassy mineral content included quartz and mullite for the Class F fly ash and quartz, anhydrite, periclase, anhydrite and magnetite for the Class C fly ash. Silica fume was a commercial compacted product having SiO_2>93.8%. X-ray diffraction (XRD) indicated the absence of crystalline components. Scanning electron microscopy indicated that the silica fume consisted of clusters of about 25-μm particles size that were composed of many small spherical particles approximately 1 μm in diameter. Quartz flour is a powdered sand (SiO_2>98%) with a mean particle size of approximately 17 μm and a Blaine fineness of 3860 cm^2/g.

Table 1
Chemical and physical analyses of the fly ashes

Composition (wt.%)	Fly ash	
	Class F	Class C
SiO_2	64.99	37.63
CaO	7.14	25.61
Al_2O_3	20.52	19.76
Fe_2O_3	3.67	6.07
MgO	0.57	4.22
MnO	0.05	0.04
TiO_2	1.41	1.52
SrO	0.10	0.35
Na_2O	0.03	1.30
K_2O	0.92	0.32
SO_3	0.48	2.29
L.O.I. (1000 °C)	0.12	0.28
Total	100	99.39
Physical data		
Density (g/cm^3)	2.42	2.64
Blaine fineness (cm^2/g)	2640	4190

2.2. Sample preparation and analysis

Samples of Class H cement with 35% by weight addition of fly ash, silica fume or quartz flour were mixed in a Waring blender at a constant water/solid ratio of 1.35 and were placed into sets of three 2×2 in. cube molds. The molds were put in an autoclave and heated to 180 °C under 20.7 MPa pressure for 1, 3, 7 and 25 days. After curing, the samples were cooled to room temperature for 24 h and demolded. The compressive strengths of the cubes were determined using a Tinius Olsen testing machine with a Model CMH 496 controller. Pieces retained from the interior of the crushed cubes were ground to a fine powder in an agate mortar, washed in acetone and dried under suction. The phase compositions of the ground powders were determined by XRD using a Philips Model 1830 X'Pert diffractometer with CuK_α radiation.

Also prepared were additional samples in which Class H cement with fly ash or silica fume at 70:30 ratio were mixed with 35% additional quartz flour at water/solid ratio of 1.35 and cured at 180 °C and 20.7 MPa for 7 days.

3. Results

3.1. Class F fly ash

Fig. 1 shows the XRD results obtained for the Class H cement with 35% addition of Class F fly ash. The major products formed at 1 day were α-C_2SH [$Ca_2Si\ O_4.H_2O$], hydrogrossular-type phase [$Ca_3Al_2(SiO_4)(OH)_8$] and a poorly crystallized aluminum substituted tobermorite [$Ca_5Si_5\ Al(OH)O_{17}.5H_2O$]. Mullite and, possibly, hematite components of the Class F fly ash were also observed in trace amounts. Unidentified phases were also present in minor to trace amounts, with relatively strong peaks at 0.284 and 0.277 nm. Some minor changes between 1 and 3 days were apparent, with relative intensities of some of the peaks changing and formation of trace amounts of a new phase. From 3 to 7 days, no change in phase equilibrium was apparent, but a significant change did occur by 25 days. The hydrogrossular-type phase became predominant, with only minor amounts of α-C_2SH and poorly crystallized aluminum-substituted tobermorite. The amount of the unidentified phase predominated by the 0.284 nm peak also increased. Trace amounts of another unidentified phase were observed, with the strongest peak at 0.292 nm. In the case where quartz flour was added to a 70:30 ratio blend of Class H cement/Class F fly ash, the major phase at 7 days was a highly crystalline aluminum-substituted tobermorite, with minor amounts of quartz also present.

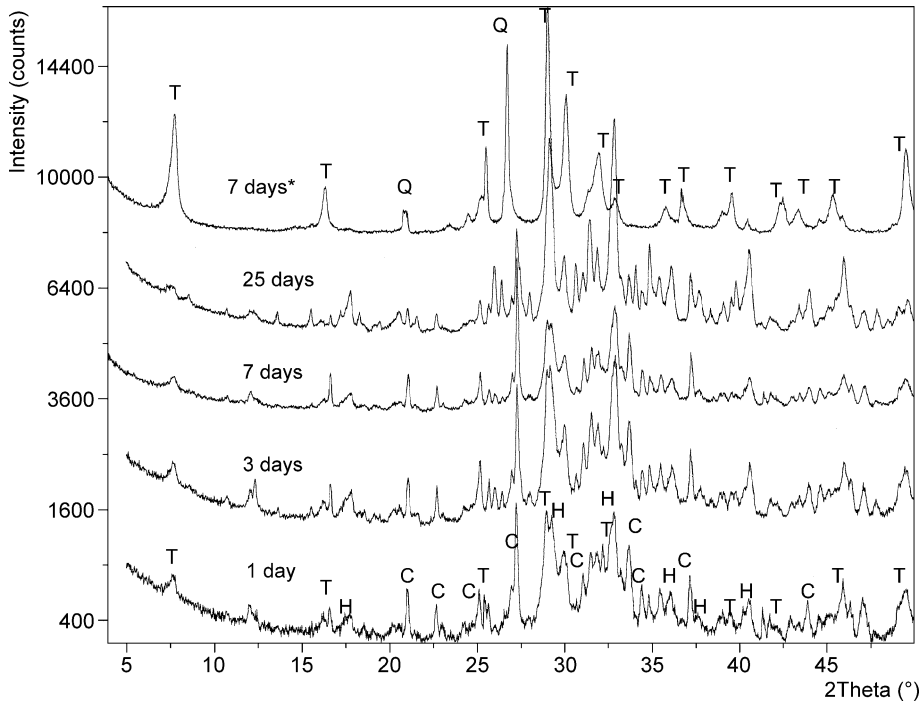

Fig. 1. XRD of Class H cement with 35% Class F fly ash(* 70:30 Class H cement/Class F fly ash with 35% quartz flour). T: tobermorite; C: α-C_2SH; H: hydrogrossular; Q: quartz.

3.2. Class C fly ash

The XRD data on the Class H cement with 35% Class C fly ash show no significant phase differences occurring between 1 and 25 days. α-C_2SH was the predominant phase formed. Minor amounts of hydrogrossular-type phase were also observed. XRD traces are given in Fig. 2. Brucite [$Mg(OH)_2$] present in the original Class C fly ash was also observed in trace amounts in the 1- to 25-day cured samples. An unidentified phase present in the trace amounts, with

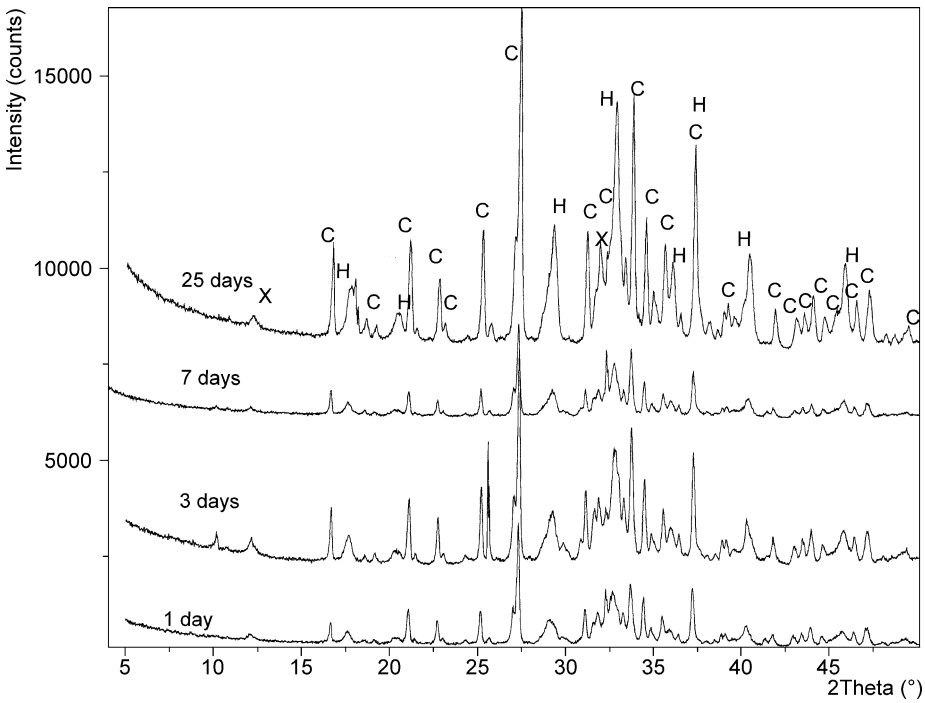

Fig. 2. XRD of Class H cement with 35% Class fly ash. C: αC_2SH; H: hydrogrossular; X: unknown phase.

strongest reflections at 0.283, 0.277 and 0.269 nm, was observed up to 25 days. Transient phases appeared to form at 3 and 7 days and disappeared by 25 days. These phases were evidenced by weak peaks at 0.869 and 0.290 nm. In addition, an indication of minute traces of quartz was noted at 3 days.

3.3. Silica fume

Fig. 3 shows the XRD data obtained for the Class H cement with the addition of 35% silica fume. As in the case with Class F fly ash, some minor phase changes occurred from 1 to 3 days, then, no noticeable changes occurred between 3 and 7 days, followed by some major changes at 25 days. The silica fume system at 1 day is predominated by the C-S-H (I) gel, with some minor phases that, as yet, have not been identified. These phases have been tentatively differentiated into a number of possible phases based on the absence or presence of peaks and changes in peak intensities obtained from the traces taken at 1, 3, 7 and 25 days. Data are provided in Table 2. The most notable change at 3 and 7 days is the presence of trace amounts of α-C_2SH. At 25 days, the phases appear to be significantly more crystalline. α-C_2SH is now a major phase, as is the unidentified Phase 2. The two primary peaks at 0.304 and 0.279 nm associated with C-S-H (I) at earlier curing times still predominate, but are very sharp, indicating transformation to a crystalline phase. Furthermore, the C-S-H (I) peak at 0.182 nm is no longer present. Minor amounts of a new phase are also observed, and the data are listed in Table 3.

Table 2
X-ray data for unidentified phases observed with silica fume

Phases observed at 1 to 7 days					
Phase 1		Phase 2		Phase 3	
d Spacing (nm)	Relative intensity	d Spacing (nm)	Relative intensity	d Spacing (nm)	Relative intensity
0.742	w	0.348	m	0.249	m
0.509	w	0.284	s	0.222	w
0.479	w	0.281	s	0.218	m
0.434	w	0.252	s	0.199	m
0.392	w				
0.265	m				
0.260	w				
0.237	w				
0.228	w				
0.210	w				
0.203	w				
0.196	w				
0.193	w				
0.185	m				

w = weak, m = medium, s = strong.

These unidentified phases do not appear to conform to typical high-temperature calcium silicate hydrates, and further investigations are underway to determine their phase composition. The addition of quartz flour to a 70:30 ratio blend of Class G cement/silica fume, however, gave only crystalline tobermorite, with trace amounts of quartz as the major phase, at 7 days. In this case, no unidentified phases were observed.

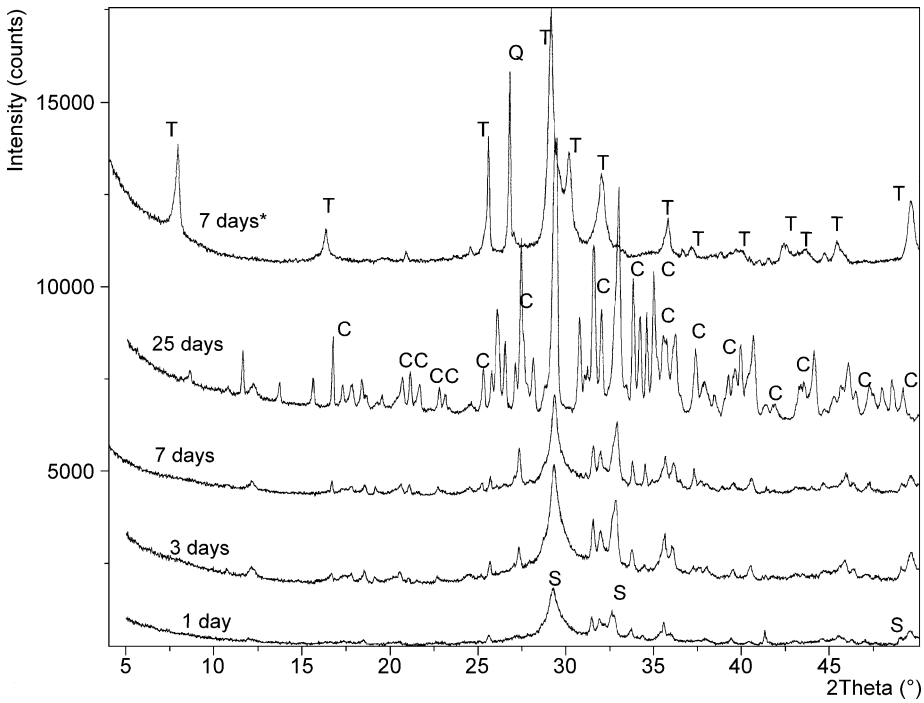

Fig. 3. XRD of Class H cement with 35% silica fume (* 70:30 Class H cement/silica fume with 35% quartz flour). T: tobermorite; C: α-C_2SH; S: C-S-H (1) gel; Q: quartz.

Table 3
X-ray data for unidentified phase observed with silica fume at 25 days

Phase 4					
d Spacing (nm)	Relative intensity	d Spacing (nm)	Relative intensity	d Spacing (nm)	Relative intensity
0.761	w	0.484	w	0.226	s
0.721	w	0.363	w	0.222	s
0.643	w	0.342	s	0.206	s
0.567	w	0.318	m	0.201	w
0.514	w	0.291	s		
0.499	w	0.263	s		

w = weak, m = medium, s = strong.

3.4. Quartz flour

The Class H cement with 35% additional silica gave primarily C-S-H(1) and poorly crystalline 1.1 nm tobermorite at 1 day, with trace amounts of xonotlite [$Ca_6Si_6O_{17}(OH)_2$] and quartz also evident. At 3 to 25 days, xonotlite becomes the more predominant phase, with C-S-H(1) and poorly crystalline 1.1 nm tobermorite as minor to trace phases. Fig. 4 gives the XRD results.

Table 4 summarizes the phase assemblage for all the systems and gives an indication of the relative amount of each phase based on relative peak intensities.

3.5. Compressive strength

Table 5 gives the compressive strength data for the Class H cements with 35% additions of fly ash, silica fume or quartz flour. The 7-day data for the 70:30 Class H Cement/Class F fly ash and 70:30 Class H cement/silica fume with additional 35% quartz flour are also included. Class H cement with addition of 35% Class F fly ash provided some compressive strength, initially, but showed a continual decline over time. Almost no strength was obtained with the Class C fly ash, and what strength there was also diminished with time. The addition of 35% silica fume to Class H cement gave reasonable strengths during the first 3 days, but these strengths then fell rapidly, giving no strength at 25 days. In fact, the sample at 25 days just crumbled like a powder as it was being demolded. The 35% quartz flour samples had relatively good compressive strengths over the time period studies, although they showed a slight decrease from 1 to 7 days and then increased significantly to 25 days. The highest compressive strengths, however, were obtained with both the 70:30 Class H cement/Class F fly ash and 70:30 Class H cement/silica fume samples with the additional 35% silica fume at 7 days. Additionally, a reasonable correlation appears to exist between the phase composition of the samples and the compressive strength obtained. This correlation will be discussed in the next section.

4. Discussion

4.1. Class C fly ash

The results clearly show that the reaction sequence and phase assemblage in the $CaO\text{-}SiO_2\text{-}H_2O$ system are influenced by the form of siliceous material used. The phase assemblage in most cases is considered to be metastable

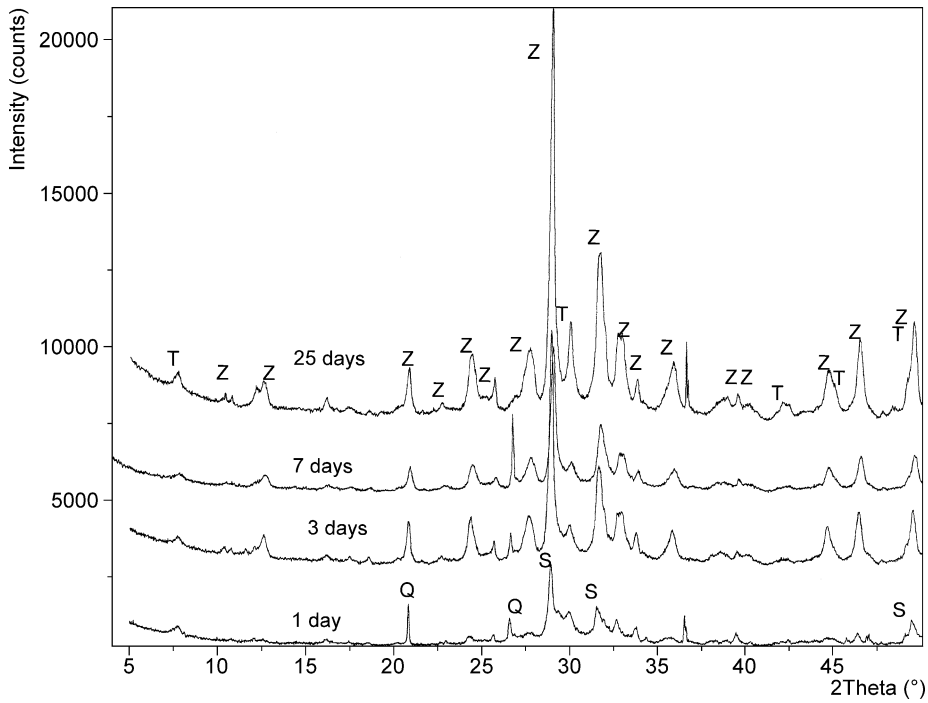

Fig. 4. XRD of Class H cement with 35% quartz flour. Z: xonotlite; T: tobermorite; S: C–S–H (1) gel; Q: quartz.

Table 4
Stable and metastable phases formed at 180 °C

Cement sample		Phases formed			
		1 Day	3 Days	7 Days	25 Days
35% Class F fly ash	Major	α-C_2SH hydrogrossular 1.1 nm Al-tobermorite	α-C_2SH hydogrossular	α-C_2SH hydogrossular	Hydogrossular
	Minor		1.1 nm Al-tobermorite	1.1 nm Al-tobermorite	α-C_2SH 1.1 nm Al-tobermorite mullite, unidentified phase (0.284 nm)
	Trace	Mullite, hematite, unidentified phase(s) (0.284 nm, 0.277 nm)	Mullite, hematite, unidentified phase(s) (0.284 nm, 0.277 nm)	Mullite, hematite, unidentified phase (0.284 nm)	Hematite unidentified phase (0.292 nm)
35% Class C fly ash	Major	α-C_2SH	α-C_2SH	α-C_2SH	α-C_2SH
	Minor	Hydrogrossular	Hydrogrossular	Hydrogrossular	Hydrogrossular
	Trace	Unidentified phase(s) (0.277 nm, 0.284 nm, 0.269 nm)	Unidentified phase(s) (0.277 nm, 0.284 nm, 0.269 nm, 0.869nm, 0.290 nm)	Unidentified phase(s) (0.277 nm, 0.284 nm, 0.269 nm, 0.869nm, 0.290 nm)	Unidentified phase(s) (0.277 nm, 0.284 nm, 0.269 nm)
35% Silica fume	Major	C-S-H (1) gel Phase 2	C-S-H (1) gel Phase 2	C-S-H (1) gel Phase 2	α-C_2SH Phase 2 C-S-H (I) gel?
	Minor	Phase 3	Phase 3	Phase 3 α-C_2SH	Phase 3 Phase 4
	Trace	Phase 1	Phase 1 α-C_2SH	Phase 1	
35% Quartz flour	Major	C-S-H (1) gel 1.1 nm tobermorite	Xonotlite	Xonotlite	Xonotlite
	Minor–trace		C-S-H (1) gel 1.1 nm tobermorite	C-S-H (1) gel 1.1 nm tobermorite	C-S-H (1) gel 1.1 nm tobermorite
70:30 Cement/ Class F fly ash[a]	Major		1.1 nm Al-tobermorite		
	Trace		Quartz		
70:30 Cement/ silica fume[a]	Major		1.1 nm tobermorite		
	Trace		Quartz		

[a] Plus 35% quartz flour.

even at 25 days. The addition of fly ash did not prevent the formation of α-C_2SH. This may be attributed to the fact that the amount of silica present was insufficient to lower the C/S ratio to that required for formation of the silica-rich phases. This was particularly true for the Class C fly ash, which, because of the intrinsic high lime content, results in a C/S ratio of 1.92, which accounts for the total CaO and SiO_2 content of the Class H cement and the Class C fly ash.

Although the Class C fly ash does lower the C/S ratio of the cement, it brings it to the C/S ratio of the α-C_2SH, and hence, this phase forms preferentially. The formation of transient phases and the unidentified minor components indicates that the total system is still in a nonequilibrium state. Although it is considered that α-C_2SH is metastable with respect to hillebrandite at 180 °C, under saturated steam pressure, there was no indication of hillebrandite forming. Pressure, however, is known to alter the phase equilibrium [1,10] and because samples were cured at 20.7 MPa no doubt helped stabilize the α-C_2SH. The low compressive strengths of 0.13 to 0.25 MPa obtained with the Class C fly ash are also consistent with the formation of α-C_2SH.

Table 5
Compressive strength of cements with 35% additions of siliceous material

Cement sample	Compressive strength (MPa)			
	1 Day	3 Days	7 Days	25 Days
35% Class F fly ash	2.70	1.48	1.49	1.22
35% Class C fly ash	0.25	0.19	0.13	0.15
35% Silica fume	4.03	3.71	1.94	0.00
35% Quartz flour	6.21	4.71	4.37	7.89
70:30 Cement/Class F fly ash[a]			11.87	
70:30 Cement/silica fume[a]			7.53	

[a] Plus 35% quartz flour.

4.2. Class F fly ash

The Class F fly ash, on the other hand, did lower the C/S ratio of the cement to approximately 1.38. At this ratio, the silica-rich phases in the $CaO-SiO_2-H_2O$ system compete with the formation of α-C_2SH. The silica-rich phase in this case is a poorly formed aluminum-substituted 1.1 nm tobermorite. Typically, most calcium silicate hydrate phases can accommodate aluminum in the structure usually in the tetrahedral sites, and 1.1 nm tobermorite is no exception [11]. In cases where pozzolanic material with a high Al_2O_3 content has been used, small amounts of hydrogarnet have sometimes been detected. In the present case, hydrogarnet was not observed. Instead, a hydrogrossular-type phase was observed. The occurrence of this phase was more prevalent

with the Class F fly ash system and was, in fact, the predominant phase at 25 days.

Compressive strengths could again be explained in relation to the phases formed. The somewhat higher 1-day strength by comparison with that of 3 and 7 days was probably due to some C-S-H(I) also being present. This phase is difficult to distinguish in a mixture with poorly crystalline tobermorite [12]. The lower compressive strength at 25 days is probably due to the more predominant hydrogrossular-type phase. The overall low compressive strength, although significantly higher than the Class C system, is most likely due to the presence of α-C_2SH. It is reported [13] that highly crystalline aluminum 1.1 nm tobermorite forms as the predominant phase in cement slag systems, with a C/S ratio less than 1.6, cured at 150 °C for 28 days and that cement Class F fly ash systems behave similarly. This report is contrary to the current findings but could relate to the difference in temperature used, as 1.1 nm tobermorite is more stable at 150 °C, whereas at 180 °C, it is considered, at least in the pure system and at atmospheric pressure, to be metastable with respect to gyrolite, truscottite and xonotlite [3].

The phase equilibria in the 70:30 ratio blend of Class H cement/Class F fly ash with additional 35% quartz flour show the effect of having sufficient silica to be in the silica-rich region of the $CaO-SiO_2-H_2O$ system. In this case, the bulk CaO and SiO_2 contents of all raw materials give a C/S of 0.64. The predominant phase in this case is a highly crystalline-aluminum-substituted 1.1 nm tobermorite, which would explain the high compressive strength obtained [4]. This is also consistent with the fact that 1.1 nm tobermorite crystallizes more rapidly at lower C/S ratio in the presence of aluminum [14]. The lower C/S also seems to favor greater substitution of aluminum in the 1.1 nm tobermorite, as no hydrogrossular-type or hydrogarnet phases were observed.

4.3. Factors controlling phase sequence

The foregoing paragraphs clearly show the effect of the C/S ratio and the influence of other components, such as aluminum, on the phase assemblage. However, given the same C/S ratio, using siliceous materials having SiO_2>97%, particle size and reactivity also seem to play a significant role in phases that form and in the phase sequence. At a bulk C/S ratio of 1.05, the addition of quartz flour favors the formation of C-S-H(1) and poorly crystalline 1.1 nm tobermorite in the short term and of xonotlite, which is considered to a stable phase at 180 °C, over the long term. Silica fume, on the other hand, formed a number of different metastable phases, some of which persisted through the 25-day curing and most of which remain unidentified. C-S-H(I) was the predominant phase at early times, with α-C_2SH forming at longer times, although the unidentified phases were not inconsequential. The formation of α-C_2SH in this silica-rich $CaO-SiO_2-H_2O$ system indicates that the important factor is not the C/S of the bulk material but the relative availability of lime and silica to the system [5,6].

The readily available silica apparently stabilizes the C-S-H(I) to the higher temperatures and possibly generates some silica-rich phases. It is assumed that the incongruent dissolution of these silica-rich phases leads to a lime-rich solution and, hence, to the formation of α-C_2SH. The formation of C-S-H and α-C_2SH as the predominant phase in silica fume systems at 180 and 200 °C has previously been observed [14]. The 1- and 3- day compressive strengths observed in the silica fume system can be attributed primarily to the C-S-H(I). The lower values in relation to quartz flour systems are most likely due to the unidentified minor phases. The formation of α-C_2SH clearly relates to the decline in compressive strength, and the total lack of any cohesion observed at 25 days suggests no binding capabilities in the other crystalline phases formed.

Interestingly, the addition of quartz flour to the system generated 1.1 nm tobermorite, again associated with a high strength. In this case, the bulk C/S was 0.5. Typically, in the presence of an active form of silica, this C/S would have been expected to favor formation of gyrolite, truscottite or a gyrolite/truscottite intergrowth. Clearly, some interesting phase relationships occurring in the silica fume system need further investigation.

5. Conclusions

Class H oil-well cement, with addition of 35% siliceous material, autoclaved at 180 °C and 20.7 MPa pressure for 1, 3, 7 and 25 days showed differences in the stable and metastable phases formed. The 70:30 Class H cement/Class F fly ash and 70:30 Class H cement/silica fume plus 35% quartz flour were also investigated. In most cases, phase equilibrium had not been attained, even at 25 days. The availability of silica and lime appears to be as significant as the bulk C/S ratio of the combined raw materials in defining what phases ultimately form. α-C_2SH, which is typically associated with the lime-rich region of the $CaO-SiO_2-H_2O$ system, formed in the silica-rich systems with C/S 1.05. Crystalline 1.1 nm tobermorite formed only as a predominant phase when the C/S ratio was less than 0.8. The only stable phase in the $CaO-SiO_2-H_2O$ system that formed was xonotlite, and this only occurred when quartz flour was used. The phase assemblage with silica fume without additional quartz flour produced a number of unidentified phases as yet to be determined. The compressive strengths appeared to correlate well with the phase assemblage and typically were highest with 1.1 nm tobermorite, somewhat lower with xonotlite and significantly lower with α-C_2SH.

References

[1] R.I. Harker, Dehydration series in the system $CaSiO_3-SiO_2-H_2O$, J. Am. Ceram. Soc. 47 (1964) 521–529.

[2] G.O. Assarsson, Hydrothermal reactions of calcium hydroxide-quartz at 120–220°, J. Phys. Chem. 64 (1958) 328–331.
[3] R.B. Peppler, The system of lime, silica, and water at 180 °C, J. Res. Natl. Bur. Stand. 54 (4) (1955) 205–211.
[4] L.H. Eilers, E.B. Nelson, L.K. Moran, High temperature cement compositions pectolite, scawtite, truscottite or xonotlite which do you want, SPE Paper 9286, 1980.
[5] K. Luke, H.F.W. Taylor, G.L. Kalousek, Some factors affecting formation of truscottite and xonotlite at 300–350 °C, Cem. Concr. Res. 11 (2) (1981) 197–203.
[6] K. Luke, H.F.W. Taylor, Equilibria and non-equilibria in the formation of xonotlite and truscottite, Cem. Concr. Res. 14 (5) (1984) 657–662.
[7] C.A. Langton, E.L. White, M.W. Gruzteck, D.M. Roy, High temperature cements with geothermal applications, Proc. 8th Int. Congr. Chem. Cements, Paris 1980, pp. V-145–V-151 Editions Septima, Paris, France.
[8] C.A. Menzel, Strength and volume change in steam cured portland cement, J. ACI 31 (1934) 31–34.
[9] L.H. Eilers, L. Root, Long-term effects of high temperature on strength retrogression of cements, SPE Paper 5028 (1974).
[10] H.F.W. Taylor, The calcium silicate hydrates, 5th ISCC II (1968) 1–27.
[11] S. Komarneni, R. Roy, D.M. Roy, C.A. Fyfe, C.J. Kennedy, Al-substituted tobermorite—the coordination of aluminum as revealed by solid-state ^{27}Al imaging angle spinning (MAS) NMR, Cem. Concr. Res. 15 (4) (1985) 723–728.
[12] J. Alexanderson, Relation between structure and mechanical properties of autoclaved aerated concrete, Cem. Concr. Res. 9 (4) (1979) 507–514.
[13] B. Drochon, M. Michaux, Cements containing high-silica minerals for well cementing, International Patent WO 03/087010, 2003.
[14] T. Mitsuda, H.F.W. Taylor, Influence of aluminium on the conversion of calcium silicate hydrate gels into 11 Å tobermorite at 90 °C and 120 °C, Cem. Concr. Res. 5 (3) (1975) 203–210.